

Molecular characterization of G-protein-coupled receptor (GPCR) and protein kinase A (PKA) cDNA in *Perinereis aibuhitensis* and expression during benzo(a)pyrene exposure

Huang Yi^{Equal first author, 1}, Sun Jia^{Equal first author, 1}, Han Ping¹, Zhao Heling², Wang Mengting¹, Zhou Yibing¹, Yang Dazuo¹, Zhao Huan^{Corresp. 1}

¹ Key Laboratory of Marine Bio-Resources Restoration and Habitat Reparation in Liaoning Province, Dalian Ocean University, Dalian, Liaoning, China

² Asian Herpetological Research Editorial Office, Chengdu Institute of Biology, Chinese Academy of Sciences, Cheng du, Sichuan, China

Corresponding Author: Zhao Huan
Email address: zhaohuan@dloou.edu.cn

Background. G-protein-coupled receptors (GPCRs) are one of the most important molecules that transfer signals across the plasma membrane, and play central roles in physiological systems. The molecular architecture of GPCRs allows them to bind to diverse chemicals, including environmental contaminants.

Methods. To investigate the effects of benzo(a)pyrene (B[a]P) on GPCR signaling, GPCR and the protein kinase A (PKA) catalytic subunit of *Perinereis aibuhitensis* were cloned. The expression patterns of these two genes during B(a)P exposure were determined with real-time fluorescence quantitative PCR. The PKA content in *P. aibuhitensis* under B(a)P exposure was examined

Results. The full-length cDNAs of *PaGPCR* and the *PaPKA* catalytic subunit were 1,514 and 2,662 nucleotides, respectively, encoding 338 and 350 amino acids, respectively. Multiple sequence alignments indicated that the deduced amino acid sequence of *PaGPCR* shared a low level of similarity with the orphan GPCRs of polychaetes and echinoderms, whereas *PaPKA* shared a high level of identify with the PKA catalytic subunits of other invertebrates. B(a)P exposure time-dependently elevated the expression of *PaGPCR* and *PaPKA*. The expression of both *PaGPCR* and *PaPKA* was also dose-dependent, except at a dose of 10 µg/L B(a)P. The PKA content in concentration group was elevated on day 4, with time prolonging the PKA content was down-regulated to control level.

Discussion. These results suggested that GPCR signaling in *P. aibuhitensis* was involved in the polychaete's response to environmental contaminants.

1

2 Molecular characterization of G-protein-coupled receptor (GPCR) and protein

3 kinase A (PKA) cDNA in *Perinereis aibuhitensis* and expression during

4 benzo(a)pyrene exposure

5

6

7 Huang Yi¹, Sun Jia¹, Han Ping¹, Zhao Heling², Wang Mengting¹, Zhou Yibing¹, Yang Dazuo¹,8 Zhao Huan¹

9

10

11 ¹Key Laboratory of Marine Bio-Resources Restoration and Habitat Reparation in Liaoning
12 Province, Dalian Ocean University, Dalian, Liaoning, China13 ²Asian Herpetological Research Editorial Office, Chengdu Institute of Biology, Chinese
14 Academy of Sciences, Chengdu, Sichuan, China

15

16

17 Corresponding Author:

18 Zhao Huan¹

19 Shahekou District heroitte street no.52, Dalian, Liao ning, 116023, China

20 Email address: 15206936767@163.com

21

22 **Abstract**23 **Background.** G-protein-coupled receptors (GPCRs) are one of the most important molecules
24 that transfer signals across the plasma membrane, and play central roles in physiological
25 systems. The molecular architecture of GPCRs allows them to bind to diverse chemicals,
26 including environmental contaminants.

27 **Methods.** To investigate the effects of benzo(a)pyrene (B(a)P) on GPCR signaling, GPCR and
28 the protein kinase A (PKA) catalytic subunit of *Perinereis aibuhitensis* were cloned. The
29 expression patterns of these two genes during B(a)P exposure were determined with real-time
30 fluorescence quantitative PCR. The PKA content in *P. aibuhitensis* under B(a)P exposure was
31 examined.

32 **Results.** The full-length cDNAs of *PaGPCR* and the *PaPKA* catalytic subunit were 1,514 and
33 2,662 nucleotides, respectively, encoding 338 and 350 amino acids, respectively. Multiple
34 sequence alignments indicated that the deduced amino acid sequence of PaGPCR shared a low
35 level of similarity with the orphan GPCRs of polychaetes and echinoderms, whereas PaPKA
36 shared a high level of identify with the PKA catalytic subunits of other invertebrates. B(a)P
37 exposure time-dependently elevated the expression of *PaGPCR* and *PaPKA*. The expression of
38 both *PaGPCR* and *PaPKA* was also dose-dependent, except at a dose of 10 µg/L B(a)P. The
39 PKA content in concentration group was elevated on day 4, with time prolonging the PKA
40 content was down-regulated to control level.

41 **Discussion.** These results suggested that GPCR signaling in *P. aibuhitensis* was involved in the
42 polychaete's response to environmental contaminants.

43 Introduction

44 Benzo(a)pyrene (B(a)P), a kind of polycyclic aromatic hydrocarbon (PAH), can cause genetic
45 damage, immune and endocrine dysfunction, and malformation in humans and other organisms.
46 Its high lipophilicity allows it to absorb to organic matter and other particulate matter and thus
47 accumulate in sediments. Recent increases in offshore oil production and transportation and the
48 sewerage discharge of domestic and industrial wastewater have led to environmental pollution in
49 coastal regions, and B(a)P has been widely detected in sediments around the world, even in
50 China. The levels of B(a)P in the sediments of Dalian Bay vary from 10.5 to 3421.2 ng/g (Zhang,
51 2008), and in the sediments around the drilling platform in the Bohai Sea, the concentration of
52 B(a)P is up to 27.69 ng/g (Yang et al, 2016). PAH such as B(a)P can be absorbed by benthic
53 organisms via ingestion or through their body surfaces, and B(a)P is reported to have serious
54 effects on deposit feeders. Therefore, the toxicity and bioavailability of B(a)P are important
55 factors in the assessment of sediment pollution.

56 G-protein-coupled receptors (GPCRs) are the largest superfamily of cellmembrane proteins
57 (Fredriksson et al, 2003). The molecular architecture of the GPCRs allows them to bind to
58 diverse organic and inorganic molecules. GPCRs mediate cell proliferation and survival by
59 transmitting signals from a range of extracellular ligands across the cell membrane to signaling
60 pathways. In vertebrates, they are key regulators of the innate and adaptive immune responses
61 and have been investigated as potential targets in drug discovery (Garland, 2013). However,
62 examples of GPCRs in invertebrates are limited. Miller et al. (2015) reported that
63 *Caenorhabditis elegans* with mutations in the GPCR follicle-stimulating hormone receptor 1
64 (FSHR-1) died significantly more quickly in the presence of cadmium than wild-type nematodes,
65 which suggests that this GPCR pathway protects the nematode against cadmium-induced

66 damage. They also found that FSHR-1 antagonizes the capacity of *C. elegans* to resist cold
67 stress, and the mutants lacking *fshr-1* survived better than wild-type worms at low temperatures.
68 *Dong and Zhang (2012)* identified a putative GPCR gene, *HPIR*, in the red swamp crayfish
69 *Procambarus clarkia*, and the expression of *HPIR* was significantly increased in the presence of
70 Gram-negative bacteria.

71 Because the aromatic structures present a number of GPCR ligands, GPCRs are potential
72 targets of aromatic pollutants such as B(a)P (*Ferrec and Ovrevik, 2018*). *Mayati et al. (2012)*
73 reported the interaction between B(a)P and the β_2 -adrenergic receptor (β_2 ADR) in endothelial
74 HMEC-1 cells and the consequent increase in intracellular Ca^{2+} , which influenced the expression
75 of cytochrome P450 B1. This suggests that β_2 ADR, a kind of GPCRs, is potentially involved in
76 the deleterious effects of B(a)P. *Factor et al. (2011)* also observed the reduced expression and
77 function of β_2 ADR in airway epithelial cells and smooth muscle cells after their exposure to a
78 mixture of PAHs. This implies that the β_2 ADR signal transduction pathway is affected by PAHs.
79 These data indicate that PAHs, including B(a)P, modulate the concentrations of intracytosolic
80 cyclic adenosine monophosphate (cAMP) or Ca^{2+} via G-protein-dependent mechanisms (*Bainy,*
81 *2007; Nadal et al., 2000*).

82 The marine polychaete *Perinereis aibuhitensis* is widely distributed in the mudflats and
83 estuarine sediments that occur widely along the coasts of Southeast Asia. They spend most of
84 their lives within the sediments, ensuring their continuous contact with any sediment-associated
85 contaminants. *Chen et al. (2012)* identified a *CYP4* gene of *P. aibuhitensis* and showed that
86 exposure to petroleum hydrocarbons significantly induced the expression of this gene. To clarify
87 whether GPCR signal transduction pathway was involved in modulating the toxicity of aromatic
88 pollutants, the full-length *GPCR* and protein kinase A (*PKA*) cDNAs were cloned and the
89 expression patterns of these two genes were determined in this study. Our results provide
90 important information on the function of GPCRs in polychaetes.

91 **Materials & Methods**

92 **B(a)P exposure**

93 *Perinereis aibuhitensis* specimens (10–15 cm, 2.0 ± 0.5 g wet weight) were collected from
94 Dalian Dongyuan aquaculture farm at the estuary of Jinzhou Bay in Dalian, China. we have a
95 long term cooperation agreement with the farm. The agreement permits us to collect research
96 samples from all their aquaculture sites including a certain estuary area under their ownership
97 (The field permit is attached in supplemental files). The animals were transferred to the
98 laboratory and acclimatized in filtered seawater (salinity 31–32, temperature $16 \pm 0.5^\circ\text{C}$) for a
99 week before the experiment. During acclimatization, the *P. aibuhitensis* were fed a powdered
100 mix containing kelp powder, gulf-weed powder, fish meal, yeast, and spirulina powder. The
101 worms were deprived of food during their exposure to B(a)P.

102 Based on the standard seawater quality of the People's Republic of China (GB 3097-1997),
103 four B(a)P concentration groups were established: 0.5, 5, 10, and 50 $\mu\text{g/L}$. A blank (seawater
104 only) group and an acetone control group (100 $\mu\text{L/L}$) were also established. Three repetitions of

105 each concentration group were set up. Ten worms were randomly placed in 2L beakers
106 containing different concentrations of B(a)P. During the experiment, the temperature of the
107 seawater was $16 \pm 0.5^\circ\text{C}$, and the seawater was renewed every 24h. On days 4, 7, and 14 of the
108 experiment, four individuals were randomly sampled from each concentration group, and the
109 body wall was removed for gene expression analysis. Three individuals was randomly sampled
110 for PKA content analysis.

111 **Cloning the full-length *GPCR* and *PKA* cDNAs of *P. aibuhitensis***

112 Three worms in blank group were ground to powder and the total RNA was extracted with
113 RNAiso™ Plus (TaKaRa, Dalian, China). The quality of the RNA was determined with 1%
114 agarose gel electrophoresis. The RNA (500 ng) was reverse transcribed to cDNA for the rapid
115 amplification of cDNA ends (RACE) using the SMARTer® RACE Kit (Clontech, Palo Alto,
116 CA, USA). The 3' and 5' RACE primers were designed with the Primer 5.0 software (PREMIER
117 Biosoft, Palo Alto, CA, USA) according to the confirmed partial sequences of *GPCR* and *PKA*
118 obtained from *P. aibuhitensis* transcriptome sequences in our laboratory (unpublished). The
119 primers used in this study are shown in Table 1.

120 The 3' RACE amplification of *P. aibuhitensis GPCR* (*PaGPCR*) was performed using the 3'
121 RACE cDNA as the template. The PCR system (50 μL) for *PaGPCR* contained 15.5 μL of PCR-
122 grade water, 25.0 μL of 2 \times SeqAmp Buffer, 1.0 μL of SeqAmp DNA polymerase, 2.5 μL of 3'
123 RACE cDNA, 5.0 μL 10 \times UPM (universal primer mixture), and 1.0 μL of primer GPCR-F1 (10
124 μM). The thermal cycling conditions were: 35 cycles of denaturation at 94°C for 30 s, annealing
125 at 65°C for 30s, and extension at 72°C for 3 min. The 3' RACE amplification of *P. aibuhitensis*
126 *PKA* (*PaPKA*) was performed with nested PCR. The outer PCR reaction system for *PaPKA* was
127 the same as that for *PaGPCR*, except that a specific primer was used. The reaction conditions for
128 the outer PCR were: 35 cycles of denaturation at 94°C for 30 s, annealing at 63.9°C for 30 s, and
129 extension at 72°C for 3 min. The outer PCR product (5.0 μL) was diluted with 245 μL of TE
130 buffer, and 5.0 μL of the diluted product was used as the template for the inner PCR. The
131 reaction conditions and system for the inner PCR were the same as for the outer PCR of *PaPKA*.

132 The 5' RACE product of *PaGPCR* was amplified with nested PCR. The outer PCR reaction
133 system (50 μL) for *PaGPCR* contained 15.5 μL of PCR-grade water, 25.0 μL of 2 \times SeqAmp
134 Buffer, 1.0 μL of SeqAmp DNA polymerase, 2.5 μL of 5' RACE cDNA, 5.0 μL of 10 \times UPM,
135 and 1.0 μL of primer GPCR-R1 (10 μM). The reaction conditions for the outer PCR were: 35
136 cycles of denaturation at 94°C for 30 s, annealing at 60°C for 30 s, and extension at 72°C for 3
137 min. The outer PCR product (5.0 μL) of *PaGPCR* was diluted with 245 μL of TE buffer and 5.0
138 μL of the diluted product was used as the template for the inner PCR. The reaction system (50
139 μL) for the inner PCR of *PaGPCR* contained 5.0 μL of the diluted outer PCR product, 17.0 μL of
140 PCR-grade water, 25.0 μL of 2 \times SeqAmp Buffer, 1.0 μL of SeqAmp DNA Polymerase, 1.0 μL
141 of UPM Short, and 1.0 μL of primer GPCR-R2 (10 μM). The reaction conditions were: 20 cycles
142 of denaturation at 94°C for 30 s, annealing at 60°C for 30 s, and extension at 72°C for 3 min. The
143 5' RACE of *PaPKA* was amplified with ordinary PCR, and the reaction system and conditions
144 were the same as those for *PaGPCR*.

145 The PCR products were detected with 1% agarose gel electrophoresis and purified with the
146 Agarose Gel DNA Purification Kit (Tiangen, Beijing, China), according to the manufacturer's
147 instructions. The PCR products were sequenced by Takara Biotechnology Co. Ltd.

148 **Bioinformatic analysis of PaGPCR and PaPKA**

149 The amino acid sequences of *PaGPCR* and *PaPKA* were deduced with the Expert Protein
150 Analysis System (<http://www.us.expasy.org/tools>). The conserved domain in each amino acid
151 sequence was analyzed with the Motif Scan (<http://www.hits.isbsib.ch/cgi-bin/PESCAN>) and
152 Expasy (<http://www.au.expasy.org/prosite/>). The protein localization sites in the cell were
153 predicted with the Psort software (<http://psort.hgc.jp/form2.html>). The transmembrane (TM)
154 helix in the protein were predicted with the TMHMM software
155 (<http://www.cbs.dtu.dk/services/TMHMM/>). The tertiary structures of *PaGPCR* and *PaPKA*
156 were predicted with the Swiss-Model software (<http://swissmodel.expasy.org/interactive>).
157 Multiple sequences were aligned with the Clustal W software (<http://www.ebi.ac.uk/clustalW>).
158 Phylogenetic analysis of GPCR and PKA were performed in MEGA 5.0. The tree topologies
159 were evaluated with bootstrapping, using 1,000 replicates.

160 **Expression of *PaGPCR* and *PaPKA* genes during B(a)p exposure**

161 Real-time fluorescence quantitative PCR was used to investigate the expression of the two genes
162 in *P. aibuhitensis* during B(a)p exposure. The β -actin gene was used as the reference gene,
163 according to our previous study (*Li et al., 2018*). The primer information is shown in Table 1.
164 Amplification was performed in 20 μ L reaction system containing 10 μ L of SYBR Premix Ex
165 Taq II (Tli RNaseH Plus)(TaKaRa, Dalian, China), 0.8 μ L of each primer (10 μ M), 0.4 μ L of
166 50 \times ROX Reference Dye II, 2.0 μ L of cDNA, and 6.0 μ L of H₂O. The reaction conditions were:
167 95 $^{\circ}$ C for 30 s, then 40 cycles of 95 $^{\circ}$ C for 5 s and 60 $^{\circ}$ C for 34 s. The melting curves were
168 analyzed after the real-time quantitative PCR. The standard curves were tested with serial 10-
169 fold sample dilutions. The slopes of the standard curves and the PCR efficiency were calculated
170 to confirm the accuracy of the real-time PCR data.

171 **PKA content in *P. aibuhitensis* under B(a)P exposure**

172 Body wall (about 100 mg) of each sample was homogenized in 0.9 mL cold phosphate buffer
173 saline (PBS) with pH 7.4. The homogenate was centrifuged at 4 $^{\circ}$ C at 3000 rpm/min for 15 min. The
174 supernatants were assayed for PKA content using the non-radioactive PKA assay kit (Kexing,
175 shanghai, China) with the method of ELISA according to manufacturer's protocol. Results are
176 expressed as ng/mL.

177 **Statistical analysis**

178 The relative quantitative ($2^{-\Delta\Delta C_t}$) method was used to analyze the expression of the *PaGPCR* and
179 *PaPKA* genes. The data are expressed as means \pm standard deviations (SD), and one-way
180 analysis of variance was used to analyze the significance of the differences among the different
181 concentration groups at each sampling point, with the SPSS 19.0 software. *P* values ≤ 0.05 were
182 considered statistically significant.

183 **Results**

184 **Molecular characterization of *PaGPCR***

185 The 5'RACE and 3'RACE products of *PaGPCR* was 1082 bp and 800 bp, respectively (see
186 supplemental file of PCR database), and the full length cDNA of *PaGPCR* was obtained by
187 sequence assembly. The full-length cDNA of *PaGPCR* was 1,514 bp and included a 5'
188 untranslated region (UTR) of 213 bp, a 3' UTR of 284 bp, and an open reading frame (ORF) of
189 1,017 bp, encoding 338 amino acids with a predicted molecular weight of 38.799 kDa and a
190 theoretical isoelectric point of 9.38 (Figure 1). This nucleotide sequence was deposited in the
191 GenBank database under accession number KX792261. The seven-transmembrane (7TM)-helix
192 bundle (304–1,146 bp) that defines the GPCR protein family was present in *PaGPCR*. The
193 glutamic acid/aspartic acid-arginine-tyrosine (E/DRY) motif (amino acids 124–126) at the border
194 between TM III and intracellular loop 2 and the NPXXY motif (amino acids 298–302) of TM
195 VII near the inner cell membrane were detected in the deduced protein sequence, indicating that
196 the protein sequence belonged to the rhodopsin family. In an amino acid comparison, PaGPCR
197 shared 33% similarity with the orphan GPCR of *Platynereis dumerilii* and 30%–33% similarity
198 with galanin receptor type 2 of echinoderms (Figure 2).

199 The predicted cellular localization of the PaGPCR protein showed it mostly located on the cell
200 membrane (52.2%), and seven TM helices were predicted in the deduced protein sequence
201 (Figure 3). The three-dimensional structural analysis of PaGPCR showed that it contained seven
202 α -helices, similar to the GPCRs of other animals (Figure 4). Its three-dimensional structure and
203 protein localization confirmed that this protein sequence was a GPCR.

204 **Molecular characterization of *PaPKA***

205 The 5'RACE and 3'RACE products of *PaPKA* was 1918 bp and 1765 bp, respectively (see
206 supplemental file of PCR database), and the full length cDNA of *PaPKA* was obtained by
207 sequence assembly. The total length of *PaPKA* cDNA was 2662 bp, containing a 3' UTR of 1,483
208 bp, a 5' UTR of 126 bp, and an ORF of 1,053 bp encoding 350 amino acids (Figure 5). The
209 predicted molecular weight of PaPKA was 40.28 kDa and its theoretical isoelectric point was
210 8.35. The nucleotide sequence was deposited in GenBank under accession number KX839259. A
211 glycine-rich loop GTGSFGRV (amino acids 50–57), Ser/Thr active site RDLKPEN (amino acids
212 165–171), PKA-regulatory-subunit-binding site LCGTPEY (amino acids 198–204), DFG triplet
213 (Asp–Phe–Gly) for orienting the γ -phosphates of adenosine triphosphate (ATP) for transfer, APE
214 motif (Ala-Pro-Glu) to stabilize the structure of the large lobe of PKA, and conserved
215 phosphorylation site (Thr197) were detected in this deduced amino acid sequence. The presence
216 of these conserved regions indicated that *PaPKA* was the catalytic subunit of PKA. An amino
217 acid comparison indicated that PaPKA was highly similar to other PKA catalytic subunits
218 (Figure 6).

219 The predicted location of PaPKA in the cell was predominantly in the cytoplasm (47.8%). The
220 three-dimensional structural analysis of PaPKA showed that it folded into a two-lobed structure
221 (Figure 7). The small lobe had a predominantly β -sheet structure, which was responsible for
222 anchoring and orienting the nucleotide, and the large lobe had a predominantly α -helix structure,
223 and was primarily involved in binding the peptide substrate and initiating phosphotransfer

224 (*Hanks and Hunter, 1995*). Ser53, Phe54, and Gly55 formed hydrogen bonds with ATP β -
225 phosphate oxygens, and Leu49 and Val57 formed a hydrophobic pocket enclosing the adenine
226 ring of ATP.

227 **Phylogenetic analysis of PaGPCR and PaPKA**

228 Phylogenetic trees were constructed from the amino acid sequences of GPCR and PKA, (Figure
229 8 and Figure 9, respectively). Figure 8 indicates that PaGPCR shared great identity with the
230 orphan GPCRs of other polychaetes. Figure 9 shows that PaPKA shared identity with mollusk
231 PKAs, which clustered together on a single branch.

232 **Effects of B(a)P on PaGPCR and PaPKA expression in *P. aibuhitensis***

233 Figure 10A shows the expression of the *PaGPCR* gene of *P. aibuhitensis* during B(a)P exposure.
234 There was no difference in its expression between the acetone control group and the blank
235 control group, indicating that acetone as a solvent had no toxic effect on the nematodes. During
236 exposure to B(a)P, the expression of the *PaGPCR* gene increased both time- and approximately
237 dose-dependently. On day 4, *PaGPCR* expression was significantly upregulated ($P < 0.05$) in all
238 but the 0.5 $\mu\text{g/L}$ B(a)P group. The expression of *PaGPCR* in the 5, 10, and 50 $\mu\text{g/L}$ B(a)P groups
239 was 2.32-, 3.46-, and 3.15-fold higher than in the blank control group, respectively. On day 7, the
240 expression of *PaGPCR* in the 0.5, 5, 10, and 50 $\mu\text{g/L}$ B(a)P groups was 3.10-, 2.91-, 3.59-, and
241 3.28-fold higher than in the blank control group, respectively ($P < 0.05$). The expression of
242 *PaGPCR* in each concentration group reached its highest level on day 14, at 4.30-, 6.60-, 4.79-,
243 and 6.36-fold higher than the blank control group, respectively ($P < 0.01$).

244 The expression pattern of the *PaPKA* gene during B(a)P exposure was the same as that of
245 *PaGPCR* (Figure 10B). The expression of *PaPKA* increased as the time of exposure increased.
246 On day 4, the expression of *PaPKA* was slightly higher in all but the 0.5 $\mu\text{g/L}$ B(a)P
247 concentration group, at 1.79-, 1.21-, and 2.21-fold higher in the 5, 10, and 50 $\mu\text{g/L}$ B(a)P groups,
248 respectively, than in the blank control group. The expression of *PaPKA* in each concentration
249 group was higher on day 7 than on day 4, at 1.25-, 1.90-, 2.52-, and 2.89-fold higher in the 0.5, 5,
250 10, and 50 $\mu\text{g/L}$ B(a)P groups, respectively, than in the blank control group ($P < 0.05$). On day
251 14, the expression of *PaPKA* reached its highest level in each concentration group, at 3.19-, 5.03-
252 , 3.10-, and 5.02-fold higher than the blank control group, respectively ($P < 0.05$).

253 **Effect of B(a)P on PKA content in *P. aibuhitensis***

254 The PKA content in *P. aibuhitensis* under B(a)P exposure was detected (Figure 11). The PKA
255 content in each concentration group increased and reached its highest level on day 4. The PKA
256 content in each concentration group was 30.09, 34.26, 30.37 and 26.11 ng/mL, respectively, and
257 the content of PKA in 5 $\mu\text{g/L}$ B(a)P concentration group was significantly higher than in the
258 blank control group ($P < 0.05$). On day 7, the PKA content in each concentration group was
259 slightly higher than in the blank control group, but was downregulated than on day 4. The PKA
260 content in the 0.5, 5, 10, and 50 $\mu\text{g/L}$ B(a)P groups was 24.01, 24.97, 21.79 and 24.69 ng/mL,
261 respectively. On day 14, the PKA content in the 0.5, 5 and 50 $\mu\text{g/L}$ B(a)P groups was still
262 downregulated than on day 7, but the PKA content in 10 $\mu\text{g/L}$ B(a)P group was slightly

263 upregulated. The PKA content in each concentration group was 20.62, 20.90, 23.67 and 24.59
264 ng/mL, respectively.

265 Discussion

266 To investigate the relationship between GPCR signal transduction pathway and B(a)P exposure
267 in *P. aibuhitensis*, the full-length cDNAs of the *PaGPCR* and *PaPKA* were isolated and
268 characterized in *P. aibuhitensis* for the first time. The sequence of *PaGPCR* contained 1514 bp,
269 encoding 338 amino acids. The deduced protein sequence of PaGPCR contained a 7TM helix
270 bundle domain, flanked by the extracellular N-terminal region and the intracellular C-terminus.
271 As part of the functional mechanism of GPCR, the E/DRY motif (amino acids 124–126), which
272 plays an important role in regulating the conformational state of GPCR, occurred at the border
273 between TM III and intracellular loop 2 in this sequence. The protein sequence of PaGPCR also
274 contained the NPXXY motif (amino acids 298–302) in TM VII, which confirmed that it
275 belonged to the rhodopsin family, the largest of the five families involved in many signaling
276 processes (Fredriksson *et al.*, 2003). A multiple protein sequence alignment showed that
277 PaGPCR shared almost 33% homology with the galanin receptor of echinoderms. A
278 phylogenetic analysis showed that it clustered most closely with the orphan GPCRs of other
279 polychaetes, and the galanin receptor of echinoderms. It is well-known that proteins with similar
280 sequences often display comparable functions if the sequence identity exceeds 30% (Kakarala
281 and Jamil, 2014). However, the short transmembrane sequences showed relative low e values
282 with other GPCRs. If the e-values are low, a prediction based on sequence identity and three
283 dimension structural analysis may not be reliable. Therefore, further study for investigating
284 ligand receptor binding is needed to prove the function of PaGPCR. In contrast to the low
285 sequence identity of GPCR, PKA in *P. aibuhitensis* shared high sequence identity with the PKA
286 catalytic subunits of other species. *PaPKA* contained 2,662 bp, which encoded 350 amino acids.
287 The deduced amino acid sequence of PaPKA contained all the conserved domains that were
288 necessary for kinase activity, such as the conserved Thr in the activation loop, the ATP-binding
289 site (GTGSFGRV), the serine/threonine kinase active site (RDLKPEN), and the PKA-
290 regulatory-subunit-binding site (LCGTPEY). The highly conserved amino acids at the ATP-
291 binding site played important roles in ATP binding and phosphotransfer. The high homology
292 among the PKA catalytic subunits suggested that they have a conserved role in intracellular
293 signaling in both vertebrates and invertebrates.

294 GPCRs comprise the largest and most important family of cell-surface proteins, transmitting
295 signals from extracellular ligands. In vertebrates, they are key regulators of the innate and
296 adaptive immune responses and have been used as potential targets in drug discovery (Garland,
297 2013). However, they have been inadequately investigated in invertebrates. Miller *et al.* (2015)
298 reported that FSHR-1 mutants of *C. elegans* died significantly more quickly during cadmium
299 exposure than wild-type nematodes, which suggests that the GPCR pathway protects *C. elegans*
300 against pollutant damage. Dong and Zhang (2012) reported that Gram-negative bacterial
301 infection induced the expression of the *HP1R* gene in *Procambarus clarkia*. Those results in
302 invertebrates indicate GPCR may also play important role in immune response to environment

303 stimulation. In the present study, we found that B(a)P exposure induced the expression of
304 *PaGPCR*, which increased with time in each concentration group. This result implied that GPCR
305 may play an important role in reducing the deleterious effects of B(a)p in *P. aibuhitensis*. GPCRs
306 interact with diverse chemical structures, which increases cAMP production, which then
307 stimulates phospholipase C activity and the subsequent mobilization of Ca^{2+} . *Mayati et al.*
308 (2012) observed an interaction between B(a)P and β_2 ADR in endothelial HMEC-1 cells, which
309 altered the levels of intracellular Ca^{2+} and the expression of cytochrome P450 B1. *Factor et al.*
310 (2011) observed the reduced expression and function of β_2 ADR in airway epithelial cells and
311 smooth muscle cells after their exposure to a mixture of PAHs. In the present study, we observed
312 that the expression of *PaPKA* in *P. aibuhitensis*, was higher during B(a)P exposure than the
313 control level in all but the 0.5 μ g/L B(a)p concentration group. The expression of *PaPKA* was
314 significantly and exposure-time-dependently induced by 50 μ g/L B(a)P. Besides the gene
315 expression of *PaPKA*, the PKA content was also detected in this study, the PKA content in *P.*
316 *aibuhitensis* under B(a)P exposure was upregulated on day 4. Kreiling et al. (2004) reported
317 exposure to a mixture of bromoform, chloroform and tetrachloroethylene increased cAMP-
318 dependent protein kinase in *Spisulula solidissima* embryos. PKA was implicated in regulation of
319 invertebrate haemocyte activity as well as humoral immune response. The increase of PKA
320 combined with GPCR indicated that GPCR pathway in *P. aibuhitensis* was affected by PAHs.
321 After day 4 the PKA content in B(a)P concentration group still higher than in the blank control
322 group, but was downregulated compared to day 4. However, the gene expression of *PaPKA* was
323 time-dependent, the inconsistency of gene expression and protein content showed that there is no
324 simple linear relationship between transcription and translation levels. We speculated that during
325 short time exposure (4 day), the metabolic detoxification in *P. aibuhitensis* was significantly
326 upregulated in order to reduce the toxic effect of PAHs. With time prolonging the organism tends
327 to homeostasis, so the PKA content was not increased continuously.

328 B(a)P can be metabolized by organisms through a series of enzymatic and nonenzymatic
329 reactions. Typically, B(a)P is metabolized by the phase I enzyme cytochrome P450 (CYP) and
330 phase II enzymes such as glutathione S-transferase (GST). The induction of CYP gene
331 expression has been detected in *P. aibuhitensis* (*Chen et al., 2012; Zhao et al., 2014*). In
332 vertebrates, the induction of the CYP enzymes involved in the biotransformation of PAHs is
333 mediated by the aryl hydrocarbon receptor (AhR) pathway. Both α - and β -type AhR proteins
334 have been reported in bivalves (*Fabbri and Capuzzo, 2010*). However, no AhR homologues have
335 been identified in other invertebrates, including marine polychaetes (*Jorgensen et al., 2008*).
336 *Ferrec and Ovrevik (2018)* reported that a number of GPCR ligands contain aromatic structures,
337 and that B(a)p modulates the concentration of intracytosolic cAMP through the GPCR pathway
338 without the involvement of conventional nuclear receptors. In this study, we demonstrated the
339 induction of *GPCR* and *PKA* expression during B(a)p exposure, so we hypothesized that the
340 GPCR pathway is also involved in the biotransformation of PAHs in *P. aibuhitensis*. Further
341 study of the relationship between GPCR and CYP expression is required to test our hypothesis.
342

343 Conclusions

344 GPCR represents a critical point of contact between cells and their surrounding environments.
345 This is the first study in which *P. aibuhitensis* GPCR and PKA cDNAs have been cloned. We
346 have also demonstrated that the expression of *GPCR* and *PKA* was induced in *P. aibuhitensis* by
347 B(a)p exposure, and that their expression was affected, to some extent, by the B(a)p
348 concentration and the exposure time. These results should be useful in investigating the
349 biotransformation of PAHs by marine polychaetes.

350 Acknowledgements

351 This work was funded by the National Natural Science Foundation of China (No. 41306138), the
352 key laboratory of mariculture and stock enhancement in North China's Sea, Ministry of
353 Agriculture and Rural Affairs, Dalian Ocean University, P. R. China(2018-KF-15) and Liaoning
354 Scientific instrument sharing Platform(L201810).

355 References

- 356 **Bainy AC. 2007.** Nuclear receptors and susceptibility to chemical exposure in aquatic
357 organisms. *Environment International* **33(4)**:571-575 DOI 10.1016/j.envint.2006.11.004
- 358 **Chen X, Zhou YB, Yang DZ, Zhao H, Wang LL, Yuan XT. 2012.** CYP4 mRNA expression in
359 marine polychaete *Perinereis aibuhitensis* in response to petroleum hydrocarbon and
360 deltamethrin. *Marine Pollution Bulletin* **64(9)**:1782-1788 DOI
361 10.1016/j.marpolbul.2012.05.035
- 362 **Dong C, Zhang P. 2012.** A putative G protein-coupled receptor involved in innate immune
363 defense of *Procambarus clarkii* against bacterial infection. *Comparative Biochemistry and*
364 *Physiology A Molecular and Integrative Physiology* **161(2)**:95-101 DOI
365 10.1016/j.cbpa.2011.09.006
- 366 **Fredriksson R, Malin CL, Lundin LG, Helgi BS. 2003.** The G-protein-coupled receptors in
367 the human genome form five main families. *Molecular Pharmacology* **63(6)**:1256-1272 DOI
368 10.1124/mol.63.6.1256
- 369 **Factor P, Akhmedov AT, McDonald JD, Qu A, Wu J, Jiang H, Dasgupta T, Panettieri Jr**
370 **RA, Perera F, Miller RL. 2011.** Polycyclic aromatic hydrocarbons impair function of b2-
371 adrenergic receptors in airway epithelial and smooth muscle cells. *American Journal of*
372 *Respiratory Cell and Molecular Biology* **45(5)**:1045-1049 DOI 10.1165/rcmb.2010-0499OC
- 373 **Fabbri E, Capuzzo A. 2010.** Cyclic AMP signaling in bivalve molluscs: an overview. *Journal*
374 *of Experimental Zoology Part A Ecological Genetics and Physiology* **313A(4)**:179-200 DOI
375 10.1002/jez.592

- 376 **Ferrec E, Øvrevik J. 2018.** G-protein coupled receptors (GPCR) and environmental exposure.
377 Consequences for cell metabolism using the β -adrenoceptors as example. *Current Opinion in*
378 *Toxicology* **8**:14-19 DOI 10.1016/j.cotox.2017.11.012
- 379 **Garland SL. 2013.** Are GPCRs still a source of new targets? *Journal of Biomolecular Screening*
380 **18**:947-966 DOI 10.1177/1087057113498418
- 381 **Hanks SK, Hunter T. 1995.** Protein kinases 6. The eukaryotic protein kinase superfamily:
382 kinase (catalytic) domain structure and classification. *The FASEB Journal* **9(8)**:576-596 DOI
383 10.1096/fasebj.9.8.7768349
- 384 **Jorgensen A, Giessing AMB, Rasmussen LJ, Andersen O. 2008.** Biotransformation of
385 polycyclic aromatic hydrocarbons in marine polychaetes. *Marine environmental* **65 (2)**:171-
386 186 DOI 10.1016/j.marenvres.2007.10.001
- 387 **Kakarala KK, Jamil K. 2014.** Sequence-structure based phylogeny of GPCR Class A
388 Rhodopsin receptors. *Molecular Phylogenetics and Evolution* **2,74**:66-96 DOI
389 10.1016/j.ympev.2014.01.022
- 390 **Kreiling JA, Stephens RE, Reinisch CL. 2005.** A mixture of environmental contaminants
391 increases cAMP-dependent protein kinase in *Spisula embryos*. *Environmental Toxicology and*
392 *Pharmacology*, **19(1)**:9-18. DOI 10.1016/j.etap.2004.02.007
- 393 **Li WJ, Xue SL, Pang Min, Yue ZH, Yang DZ, Zhou YB, Zhao H. 2018.** The expression
394 characteristics of vitellogenin(VTG) in response to B(a)p exposure in polychaete *Perinereis*
395 *aibuhitensis*. *Journal of Oceanology and Limnology* **36(06)**:399-409 DOI 10.1007/s00343-
396 019-7304-0
- 397 **Miller RL, Thompson AA, Trapella C, Guerrini R, Malfacini D, Patel N, Han GW**
398 **Cherezov V, Caló G, Katritch V, Stevens RC. 2015.** The importance of ligand-receptor
399 conformational pairs in stabilization: spotlight on the N/OFQ G protein-coupled receptor.
400 *Structure* **23(12)**: 2291-2299 DOI 10.1016/j.str.2015.07.024
- 401 **Mayati A, Levoine N, Paris H, N'Diaye M, Courtois A, Uriac P, Lagadic-Gossmann**
402 **D, Fardel O, Le Ferrec E. 2012.** Induction of intracellular calcium concentration by
403 environmental benzo(a)pyrene involves a β_2 -adrenergic receptor/adenylyl cyclase/Epac-
404 1/inositol 1,4,5-trisphosphate pathway in endothelial cells. *Journal of Biological Chemistry*
405 **287(6)**:4041-4052 DOI 10.1074/jbc.M111.319970
- 406 **Nadal A, Ropero AB, Laribi O, Maillet M, Fuentes E, Soria B. 2000.** Nongenomic actions of
407 estrogens and xenoestrogens by binding at a plasma membrane receptor unrelated to estrogen
408 receptor alpha and estrogen receptor beta. *Proceedings of the National Academy of Sciences*
409 **97(21)**:11603-11608 DOI 10.1073/pnas.97.21.11603

- 410 **Yang D, de Graaf C, Yang L, Song G, Dai A, Cai X, Feng Y, Reedtz-Runge S, Hanson**
411 **MA, Yang H, Jiang H, Stevens RC, Wang MW. 2016.** Structural determinants of binding
412 the seven-transmembrane domain of the glucagon-like peptide-1 receptor. *Journal of*
413 *Biological Chemistry* **291(25)**:12991-13004 DOI 10.1074/jbc.M116.721977
- 414 **Zhang JH. 2008.** Quality benchmark study of polycyclic aromatic hydrocarbons in marine
415 sediments. *Doctoral dissertation*. Dalian Maritime University.
- 416 **Zhao H, Zhao XD, Yue ZH, Zhou YB. 2014.** Effects of Benzo(a)pyrene on Antioxidant
417 Enzyme Activity and Cytochrome P450 Gene Expression in the *Perinereis aibuhitensis*.
418 *Journal of Dalian Ocean University* **29(4)**:342-346 DOI 10.3969/J.ISSN.2095-
419 1388.2014.04.004
- 420

Figure 1

Nucleotide sequence and deduced amino acid sequence of GPCR from *Perinereis aibuhitensis*.

Initiation codon (ATG) and termination codon (TAA) are highlighted in red boxes; The seven-transmembrane (7TM) domains (TM I to TM VII) are underlined with red lines. The E/DRY and NPXXY motifs are in shadow.

Figure 2

Multiple alignment analysis of PaGPCR with other GPCR protein.

Amino acid residues that are conserved in at least of 50% sequence are shaded and similar amino acids are shaded in dark. The GenBank accession number for these proteins are as follows: (*Platynereis dumerilii* orphan G protein coupled receptor, 56AKQ63061.1; *Strongylocentrotus purpuratus* galanin receptor type 2-like, XP_003727596.1; *Acanthaster planci* galanin receptor type 2-like, XP022098630.1; *Apostichopus japonicus* putative galanin receptor type 2-like, PIK48567.1).

```

Perinereis_aibuhitensis -----ILLHVNIMDNITFNRTFDGSLNPNFYIGDFVYVI 37
orphan_G-protein_coupled_receptor_56_Platynereis_dumerilii MAATTNVTGITTQNFNLQSEHYFETLPTQSLNVNQSAEEVDASASINFDYHLIIYYVI 60
galanin_receptor_type_2-like_Strongylocentrotus_purpuratus -----MASLNGDNLISIPMIPSPATVLTANPDQGGGGGAVLNELYLKIIYALI 50
galanin_receptor_type_2-like_Acanthaster_planci -----MAENDLPLTIIFQSIV 15
putative_galanin_receptor_type_2-like_Apostichopus_japonicus -----MDPTGFVTTGVSVYTEGIIPTSTS-----VDVLLPVLVYFI 36

Perinereis_aibuhitensis GCLGLILDNGFVIVVILHSRKMNRKLCNLEFLNQSVVDLVAVFLLCNSPSVP-----TL 91
orphan_G-protein_coupled_receptor_56_Platynereis_dumerilii GACGGIFGNILVCIWFSSATLRKKTNWFFINQSLVDFAVSPFLTVQADVQ-----GE 113
galanin_receptor_type_2-like_Strongylocentrotus_purpuratus GLLGITVGNIGVCLVFTIKRRQFQSIINNYIILNQSVIDLDSIFFLILHYASPNGPISETA 110
galanin_receptor_type_2-like_Acanthaster_planci GITGICGNALVVCVVIKIR-FMHTLNAAFENQALIDLFGSFMILLNLP-----IPD 68
putative_galanin_receptor_type_2-like_Apostichopus_japonicus GFLGLIFGNVIVVILFLANRKFVRSITNLLFLNQAIMDFVVAIFLLDRFGP-----SLYK 91

Perinereis_aibuhitensis GSASNISLEFYCRHWDSNYLFWAAVTVSTVNLVRIITERYLEVVEHPLRYSFFTRRRKRV 151
orphan_G-protein_coupled_receptor_56_Platynereis_dumerilii PPHSGIAGELYCRHWATKLFLLWGLVLSSTNVLVALTIERYLAVVHPIWHKTSFSKTRKRV 173
galanin_receptor_type_2-like_Strongylocentrotus_purpuratus NIPSRGLAEFFCRHWDSYPLWALYIASTNVLVLSLERYFATCRPVIHRNFFTVRRKRV 170
galanin_receptor_type_2-like_Acanthaster_planci PIPSNRSGVLLCRHWDSYFNLALFVSTNVLVLTIERYLAVVPPFRYQVGLTRKNALI 128
putative_galanin_receptor_type_2-like_Apostichopus_japonicus LITNETLSEMLCRHWDSYELWAFYIASTQNLVMSLERYFATCRVKKHNYFTIRGAKI 151

Perinereis_aibuhitensis IVAVVWLVGFTIPIVTSVHTSPAG-----ADGTCQKHRANSSRLMAALVGFYALFFGFLI 206
orphan_G-protein_coupled_receptor_56_Platynereis_dumerilii LIALVWLVGFPVNNASYMIVTSSNED-----GVCAIYAIWPSITVRRFFGVLTVLLQYLI 227
galanin_receptor_type_2-like_Strongylocentrotus_purpuratus AMLCVWVYGVAVYQLYWPLVQTFSA-----DWR-CHPNWPNRVVQRFMGVLLFSLEFLI 222
galanin_receptor_type_2-like_Acanthaster_planci IIVIVWVSAFLFTSYGVFIIRYK-----GQC-----KQKLVHPEVLGVAVFAVTELI 177
putative_galanin_receptor_type_2-like_Apostichopus_japonicus GIAGVWLVGLVYQSYWIVVFFEF-----SSQCFPLWNRNLTQACMGVFFVFLMEXLI 204

Perinereis_aibuhitensis PVVIMIVCVYIQMIMTFNLKVRPSDPS-----TMISESEKRRSERMLRVRRLSLIKTML 258
orphan_G-protein_coupled_receptor_56_Platynereis_dumerilii PHTFIIIFAVGSIALKLYRKLKSD-----GAAKGKDETIQRGMRNTVKTIV 272
galanin_receptor_type_2-like_Strongylocentrotus_purpuratus PPIIMTCSYVSIILMLRNRTK-----SHGKVVQNAFQRAKRNVTITL 265
galanin_receptor_type_2-like_Acanthaster_planci PVIVMLVVYAHITVVLKRGAGRIQGPAA-----AVPSTGTAPGQGESLMRARRNTFKITL 234
putative_galanin_receptor_type_2-like_Apostichopus_japonicus PPIVMTFSYVNIILMLKRR-----GQKSGS-VFQRAKRNVTITL 244

Perinereis_aibuhitensis PVVIMIVCVYIQMIMTFNLKVRPSDPS-----TMISESEKRRSERMLRVRRLSLIKTML 258
orphan_G-protein_coupled_receptor_56_Platynereis_dumerilii PHTFIIIFAVGSIALKLYRKLKSD-----GAAKGKDETIQRGMRNTVKTIV 272
galanin_receptor_type_2-like_Strongylocentrotus_purpuratus PPIIMTCSYVSIILMLRNRTK-----SHGKVVQNAFQRAKRNVTITL 265
galanin_receptor_type_2-like_Acanthaster_planci PVIVMLVVYAHITVVLKRGAGRIQGPAA-----AVPSTGTAPGQGESLMRARRNTFKITL 234
putative_galanin_receptor_type_2-like_Apostichopus_japonicus PPIVMTFSYVNIILMLKRR-----GQKSGS-VFQRAKRNVTITL 244

Perinereis_aibuhitensis MVSIVFVICWIGDQVYVFLFN--IRVIKDLQQTITTVVSLAFLNCCINBFYITCQVNDP 316
orphan_G-protein_coupled_receptor_56_Platynereis_dumerilii LVAVICFVACSWNQIYVLMNN--LGFREDYSSNFYHFTVIAVFINSCVNPMIYALKYDPP 330
galanin_receptor_type_2-like_Strongylocentrotus_purpuratus IVFVSYVVCWTPTELSLAYN--LGHVDYFESAVHDVLKGLVACNLVNBFIYAFKYEHP 323
galanin_receptor_type_2-like_Acanthaster_planci IVFVASTICWTPNEVFLFN--LGVVDNLTSTIFFVTAMVSTNSCLNBFYIYKIKYQF 292
putative_galanin_receptor_type_2-like_Apostichopus_japonicus IVFVSYVICWTPTEFGIILN--CGRPYDFEGTFHYVATVVLVLCNMTAFIYITFKYEHP 302

Perinereis_aibuhitensis QEATRLLKIKKESENERSTLDLSNQV----- 345
orphan_G-protein_coupled_receptor_56_Platynereis_dumerilii KKAAYQLFCTKMLGIRPNAIEDQS----- 354
galanin_receptor_type_2-like_Strongylocentrotus_purpuratus QSELKKIFCSMCNAGNRISTESRGTVLS PANNSNNTP----- 361
galanin_receptor_type_2-like_Acanthaster_planci RKALKTLFG--RQGGDEDESLATVATAHD----- 320
putative_galanin_receptor_type_2-like_Apostichopus_japonicus QNYLKRMFRRFCGLGNRIDVNTVSAVAEPQDQTLNRSDDTGQAATTA----- 350

```

Figure 3

Analysis of transmembrane region of PaGPCR.

The whole sequence is labeled as inside (blue line) or out side (pink line), and the transmembrane region was labeled with red line.

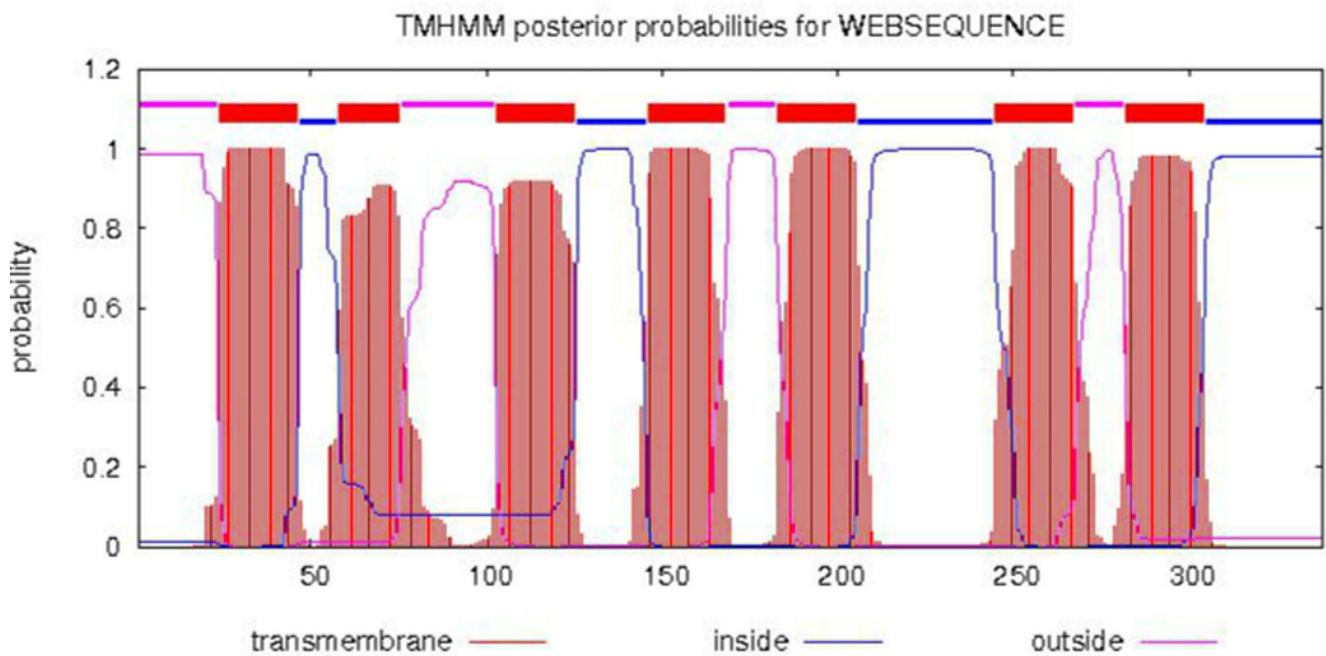


Figure 4

The three dimensional structure of PaGPCR.

The helix is colored by blue, the sheet is colored by magenta, and the loop is colored by salmon.

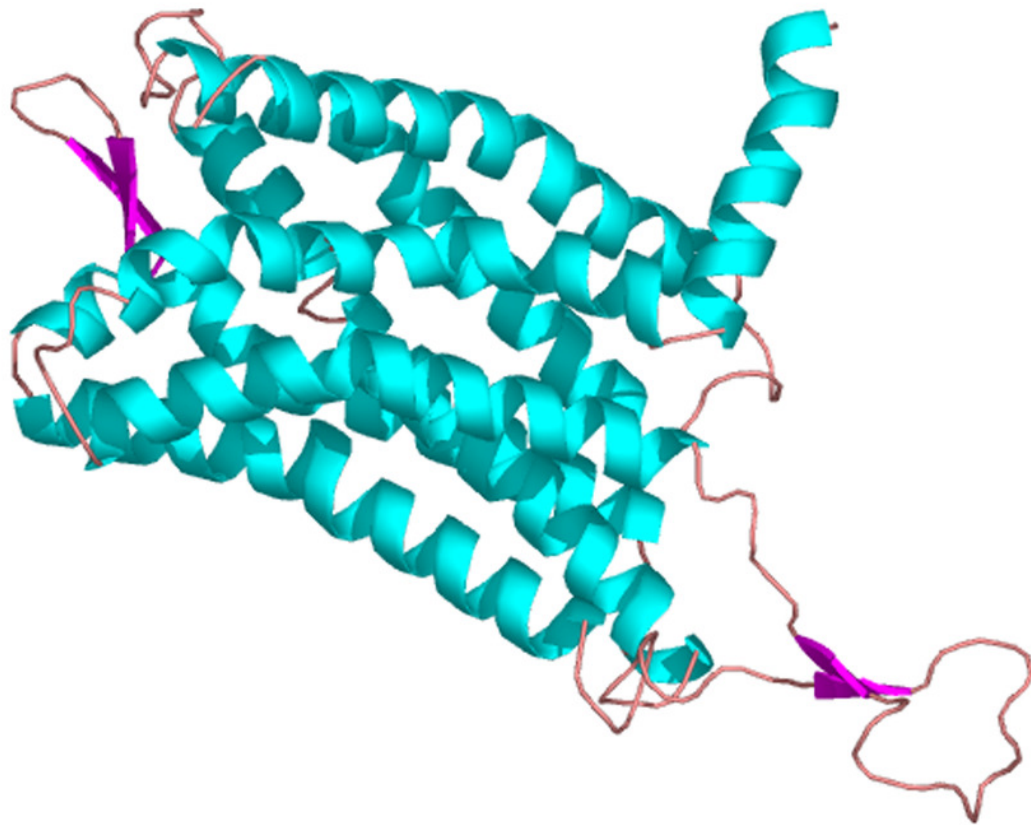


Figure 5

Nucleotide sequence and deduced amino acid sequence of PaPKA

Initiation codon (ATG) and termination codon (TGA) are highlighted in red boxes; conservative phosphorylation site, DFG triplet and APE motif are highlighted in green boxes; the glycine-rich loop GTGSFGRV (50–57aa), Ser/Thr active site RDLKPEN (165–171aa), PKA-regulatory-subunit-binding site LCGTPEY (198–204aa) are underlined with red.

```

1  GTCGAAGAGATCGAGGTGGAATATTCAGACATAATTTTTGAGAAGCTGGTCTGAGAGTTCTCTGATTTCTGGCCGGTTAATTCCTCTGGATCACCACGGACTAG
106 GTAGTTTACCACACGGTAGCCATGSGAAATGCTGCAACAGCAAAGAAAGGCGATCCAGAGAATGTCAAAGAGTTCTTAGCCAAAGCTAAAGAGGACTTCAACAAG
1  M G N A A T A K K G D P E N V K E F L A K A K E D F N K
211 AAATGGGAAGGCCATCATGTAACACTGCATCACTAGATGACTTCGACAGAATTAACCCTGGGAACAGGGTCATTGGACGGGTGATGCTGGTTCAGCACAAA
29  K W E E P S C N T A S L D D F D R I K T L G T G S F G R V M L V Q H K
316 GCCACGAAGGAGTACTATGCCATGAAGATTTTAGATAAACAAAAGGTAGTGAACACTGAAGCAAGTTGAACACACATTGAATGAAAAGAAAATTTGTCCGCCATA
64  A T K E Y Y A M K I L D K Q K V V K L K Q V E H T L N E K K I L S A I
421 TCATTTCCATTCTTAGTGAGCCTAGAGTACAGTTTTAAGGATAAECTCAAATTTGTACATGGTATTGGAGTTTCGTGACAGGAGGTGAAATGTTCTCACATCTGCGA
99  S F P F L V S L E Y S F K D N S N L Y M V L E F V T G G E M F S H L R
526 AGAATTTGGCCGATTTAGTAAAACACTCACAGCCGATTTTATGCTGCACAAGTATGCATGGTATTTGAATATCTGCACAATCTAGACACACTGTACAGAGATTTGAAG
134 R I G R F S E T H S R F Y A A Q V C M V F E Y L H N L D T L Y R D L K
631 CCAGAAAATATTCTGATTGATGACACTGGTCACTTGAGAGTAACAGACTTCGGTTTTGCCAAACGCGTAAAAGGCAGGACATGGACGTTGTGTGGCACACCCAGAG
169 P E N I L I D D T G H L R V T D F G F A K R V K G R T W T L C G T P E
736 TACCTGGCCCCAGAAATCATCTTGAGCAAGGGCTACAACAAAGCCGTAGACTGGTGGGCGCTGGAGTCCCTTGTTTATGAAATGGCAGCTGGATACCCACCTTTC
204 Y L A P E I I L S K G Y N K A V D W W A L G V L V Y E M A A G Y P P F
841 TTTGCTGACCAGCCAATCCAAATCTATGAGAAGATTGCTCAGGAAAGGTGCGCTTCCCATCTCACTTTAGTTCTGATTGAAGGATCTTTTGAAGAATCTGCTA
239 F A D Q P I Q I Y E K I V S G K V R F P S H F S S D L K D L L K N L L
946 CAGGTAGACTTGACAAAACGTTATGGAAAACCTGAAGAATGGGGTCAACGATATCAAGAATCACAAGTGGTCTCCACCACAGACTGGATTGCTATCTACCAGAAA
274 Q V D L T K R Y Y G N L K N G V N D I K N H K W F S T T D W I A I Y Q K
1051 AAGGTTGAAGCACCTTCCAAATGCAAAAGGCCAGGTGACTACAGCAACTTTGATGACTATGAGGAAGAACCACCTGAGAATTTGTCACCGGAAAAATGT
309 K V E A P F I P K C K G P G D Y S N F D D Y E E P L R I S S T E K C
1156 GCCAAGGAGTTTGACAGCTTGAAGACAGTTGGCTTGTAGGTGGCTAGTGTGTGGTGGGGAACTAAAGACTGTGATGACCATTCTGTGTTTCATGGTCTATCACT
344 A K E F A D F *
1261 GGCAGCTGGCTGAAGATCTGCGGCCACATACCACACAATCTCTCAAAGAATACATCCTTTGTGCATTAACAAATGTATATATACTTAATCATATCACATTGCGT
1366 AATTGTAACAAGGTGAATTCAGTTTCATATGTGTCAATGAGGTAAGAGAGAGGGCTTCGATCCCAGGTGTGGCATGTCCCTGAGGCTGCGCTATTTGGTCCGAGGT
1471 AAGCCAGGTCGCTTCAGCTCGCACCCAGGCTGCCTCAAAGCTACCTTGGTCGTTACTCGCCGAAGTACTCATTACCTTGCTGTGTGGCCTTCCAGATTTGT
1576 GTGGGGCAGACTGGTGGAGGATTAGGCTTTAATTGCTTTGCTGAAGTGGCCACACGGGTCCAGAAGCCAAGGCTATCTTCAAATACACAGTTAATACCATATAT
1681 TAAC TTATCATTACAACCTTACTGACCACTTGTTCACATTTAGGTCAATGTCTGCACCTTTTATTGTATACAGGTGGTCCATCTGAAACAATCTCTGAACATTTG
1786 AATTATATCCATTGTAAGGAAGTGCAAACTTCTTTGTGCTGTGCTCCTCCTCACTCCCGTGTGCTTCTTTCTCTGCTGTGAACCTTTGAATCAGAGAGAAACAA
1891 CACTTTATTTGTATGATGTCAAATATTGTACTTTTGGTAAGGCCACCTCCTAAGTGGTGGTTCATCAAGACTTGATATAGTTTGTGAGCAGTTGGCTTTTGGGT
1996 AGAGTAGGAGTTTTCTGTTCATCATACTGGTGGGATGACACCATCTCCCGCATAACAGTAGTACTGTGTAGTAGCAATAGCCGCCATAAGGCCATGAGTCTCC
2101 ATTGTTTCAGCTAATGTAGCTAGGCTTCAAGTCATAAGTCAATGATAACATATAATGGCATTATTTGTAGTACTGATGATGAGAGAATATTATCTTTGTCAAGACA
2206 AACTTATTTACTTTTATATAACTGACTTGTATGTACAGACGTC AAGGCTGTATGAACTGAGAAATTTGTTGCTTGTATGTAGTGTATAAAATGTGTATATCT
2311 ATCTCTGCATATTTTGTGTTTGTATGTCAATCCACAAATGCTTCAAATTTATCTTGAACCATGTACTTGACTAATCTAATTTGTGATTTGAAAAGGTAATTGGA
2416 GTTGTGCTGAATTAGATAGGTATGCTTCTGACATTTGTAACTACTACAGTGTGCTCCATTTGTGATGGGTCCTACTCATGAATGTTGTTATATTTGTATA
2521 TACTAAAAATAATTTATGCTGGTTCATGAAGATGTACAAAAAATATTTTTCAAATGGCTAAGGATGGTTTTGATGAAATTTGTACACTAAGGGTCAGCAGTTAA
2626 CAAACCCCATGAAAAAATAAAAAAAAAAAAAAAAAAAAAA

```

Figure 6

Multiple alignment of PaPKA with other PKA.

Amino acid residues that are conserved in at least of 50% sequence are shaded and similar amino acids are shaded in dark. The GenBank accession number for these proteins are as follows: *Aplysia californica* catalytic subunit of PKA, NP_001191420.1; *Xenopus tropicalis* cAMP dependent protein kinase catalytic subunit, NP_001164667.1; *Branchiostoma floridae* cAMP dependent protein kinase, XP_002600447.1; *Danio rerio* cAMP dependent protein kinase catalytic subunit, NP_001030148.1; *Octopus bimaculoides* cAMP dependent protein kinase catalytic subunit, XP_014777153.1; *Lingula anatina* cAMP dependent protein kinase catalytic subunit, XP_013409439.1; *Crassostrea gigas* cAMP dependent protein kinase catalytic subunit, XP_011439335.1; *Biomphalaria glabrata* cAMP dependent protein kinase catalytic subunit, XP_013072294.1; *Salmo salar* cAMP dependent protein kinase catalytic subunit, XP_014071121.1; *Gallus gallus* cAMP dependent protein kinase catalytic subunit, XP_015146370.1.

Perinereis_aibuhitensis MGNAATAK-----KGDPEEN---VKBFLAKAKBDFNKKBWEPSCNTASLDDFDRIKTLGTGSFGRVMIQVHKH-ATKEYYA 70
 Aplysia_californica MGNAATAK-----KGDPAEN---VKBFLAKAKBDFNKKBWHPASTSCLDDFDRIKTLGTGSFGRVMIQVHKHGESRNFYA 72
 Xenopus_tropicalis MGNAATAK-----KGNIEIES---VKBFLAKAKBDFLKKWBTTPPQNTASLDDFDRIKTLGTGSFGRVMIQVHKH-GAEQYYA 71
 Branchiostoma_floridae MAAKATPKGSGHGKATAIGKISKHGDGGSYSDSVKBFLAKAKBDFTKKBWSPSQNTAALDDFDRIKTLGTGSFGRVMIQVHKH-ATQNEYA 89
 Danio_riero MGNAATAK-----KGNELSES---VKBFLAKAKBDFLKKWBTTPQNTASLDDFDRIKTLGTGSFGRVMIQVHKH-ASDQYYA 71
 Octopus_bimaculoides MGNAATAK-----KGDPAEN---VKBFLAKAKBDFLKKWBTTPPQNTASLDDFDRIKTLGTGSFGRVMIQVHKH-ANKEYYA 71
 Lingula_anatina MGNAATAK-----KLDPAEN---VKAFLAQAABEFSDKWBKPSQNTAGLDDFDRIKTLGTGSFGRVMIQVHKH-QSKQYYA 71
 Crassostrea_gigas MGNAATAK-----KGDPAEN---VKBFLAKAKBDFLKKWBTTPPQNTASLDDFDRIKTLGTGSFGRVMIQVHKH-ANKDEYA 71
 Biomphalaria_glabrata MGNAATAK-----KGDPAEN---VKBFLAKAKBDFLKKWBTTPPQNTASLDDFDRIKTLGTGSFGRVMIQVHKHGENKSFYA 72
 Salmo_salar MGNAATAK-----KGNEQES---VKBFLAKAKBDFLKKWBTTPPQNTASLDDFDRIKTLGTGSFGRVMIQVHKH-GTEQYYA 71
 Gallus_gallus MGNAATAK-----KGNIEISET-VKBFLAKAKBDFLKKWBTTPPQNTASLDDFDRIKTLGTGSFGRVMIQVHKH-ATEQYYA 74

Perinereis_aibuhitensis MKILDKQKVVVKLQVEHTLNEKKILSAISFPFLVSRLEYSEKDNSNLYMVEEFVTGGEMFSLRRIIGRFSEPHSRFYAAQIVLVLFEYLHSL 160
 Aplysia_californica MKILDKQKVVVKLQVEHTLNEKKILQSIINFPFLVSRLEYSEKDNSNLYMVEEFVTGGEMFSLRRIIGRFSEPHSRFYAAQIVLVLFEYLHSL 162
 Xenopus_tropicalis MKILDKQKVVVKLQVEHTLNEKKILQAVNFPFLVSRLEYSEKDNSNLYMVEEFVTGGEMFSLRRIIGRFSEPHSRFYAAQIVLVLFEYLHSL 161
 Branchiostoma_floridae MKILDKQKVVVKLQVEHTLNEKKILQAVSFPFLVSRLEYSEKDNSNLYMVEEFVTGGEMFSLRRIIGRFSEPHSRFYAAQIVLVLFEYLHSL 179
 Danio_riero MKILDKQKVVVKLQVEHTLNEKKILQAVSFPFLVSRLEYSEKDNSNLYMVEEFVTGGEMFSLRRIIGRFSEPHSRFYAAQIVLVLFEYLHSL 161
 Octopus_bimaculoides MKILDKQKVVVKLQVEHTLNEKKILQAVSFPFLVSRLEYSEKDNSNLYMVEEFVTGGEMFSLRRIIGRFSEPHSRFYAAQIVLVLFEYLHSL 161
 Lingula_anatina MKILDKQKVVVKLQVEHTLNEKKILQAVSFPFLVSRLEYSEKDNSNLYMVEEFVTGGEMFSLRRIIGRFSEPHSRFYAAQIVLVLFEYLHSL 161
 Crassostrea_gigas MKILDKQKVVVKLQVEHTLNEKKILQAVSFPFLVSRLEYSEKDNSNLYMVEEFVTGGEMFSLRRIIGRFSEPHSRFYAAQIVLVLFEYLHSL 161
 Biomphalaria_glabrata MKILDKQKVVVKLQVEHTLNEKKILQAVSFPFLVSRLEYSEKDNSNLYMVEEFVTGGEMFSLRRIIGRFSEPHSRFYAAQIVLVLFEYLHSL 162
 Salmo_salar MKILDKQKVVVKLQVEHTLNEKKILQAVSFPFLVSRLEYSEKDNSNLYMVEEFVTGGEMFSLRRIIGRFSEPHSRFYAAQIVLVLFEYLHSL 161
 Gallus_gallus MKILDKQKVVVKLQVEHTLNEKKILQAVNFPFLVSRLEYSEKDNSNLYMVEEFVTGGEMFSLRRIIGRFSEPHSRFYAAQIVLVLFEYLHSL 164

Perinereis_aibuhitensis DLIYRDLKPENLLIDDTGHLRVTDFGFAKRVKGRWTWLCGTPEYLAPEIILSKGYNKAVDWWALGVLVYEMAAGYPPFFADQPIQIYEKI 250
 Aplysia_californica DIMYRDLKPENLLIDSYGYLKVTDGFAKRVKGRWTWLCGTPEYLAPEIILSKGYNKAVDWWALGVLVYEMAAGYPPFFADQPIQIYEKI 252
 Xenopus_tropicalis DLIYRDLKPENLLIDQQGYIQVTDGFAKRVKGRWTWLCGTPEYLAPEIILSKGYNKAVDWWALGVLVYEMAAGYPPFFADQPIQIYEKI 251
 Branchiostoma_floridae DIIYRDLKPENLLIDQLGYLKVTDGFAKRVKGRWTWLCGTPEYLAPEIILSKGYNKAVDWWALGVLVYEMAAGYPPFFADQPIQIYEKI 269
 Danio_riero DLIYRDLKPENLLIDQHGYYIQVTDGFAKRVKGRWTWLCGTPEYLAPEIILSKGYNKAVDWWALGVLVYEMAAGYPPFFADQPIQIYEKI 251
 Octopus_bimaculoides DIIYRDLKPENLLIDSSGYLKVTDGFAKRVKGRWTWLCGTPEYLAPEIILSKGYNKAVDWWALGVLVYEMAAGYPPFFADQPIQIYEKI 251
 Lingula_anatina DIMYRDLKPENLLIDSTGYLKVTDGFAKRVKGRWTWLCGTPEYLAPEIILSKGYNKAVDWWALGVLVYEMAAGYPPFFADQPIQIYEKI 251
 Crassostrea_gigas DIMYRDLKPENLLIDTMSGYLKVTDGFAKRVKGRWTWLCGTPEYLAPEIILSKGYNKAVDWWALGVLVYEMAAGYPPFFADQPIQIYEKI 251
 Biomphalaria_glabrata DLVYRDLKPENLLIDPQGYCKVTDGFAKRVKGRWTWLCGTPEYLAPEIILSKGYNKAVDWWALGVLVYEMAAGYPPFFADQPIQIYEKI 252
 Salmo_salar DLIYRDLKPENLLIDHQGYIQVTDGFAKRVKGRWTWLCGTPEYLAPEIILSKGYNKAVDWWALGVLVYEMAAGYPPFFADQPIQIYEKI 251
 Gallus_gallus DLIYRDLKPENLLIDQQGYIQVTDGFAKRVKGRWTWLCGTPEYLAPEIILSKGYNKAVDWWALGVLVYEMAAGYPPFFADQPIQIYEKI 254

Perinereis_aibuhitensis VSGKVRFPSPHFSSDLKDLLRNLLQVDLTKRYGNLKNGVNDIKHKKWFATDWTIAIYQKQVEAPFIPKCKRGGDTSNFDDYEBEEDVRISST 340
 Aplysia_californica VSGKVRFPSPHFSSDLKDLLRNLLQVDLTKRYGNLKNGVNDIKHKKWFATDWTIAIYQKQVEAPFIPKCKRGGDTSNFDDYEBEEDVRISST 342
 Xenopus_tropicalis VSGKVRFPSPHFSSDLKDLLRNLLQVDLTKRYGNLKNGVNDIKHKKWFATDWTIAIYQKQVEAPFIPKCKRGGDTSNFDDYEBEEDVRISST 341
 Branchiostoma_floridae VSGKVRFPSPHFSSDLKDLLRNLLQVDLTKRYGNLKNGVNDIKHKKWFATDWTIAIYQKQVEAPFIPKCKRGGDTSNFDDYEBEEDVRISST 359
 Danio_riero VSGKVRFPSPHFSSDLKDLLRNLLQVDLTKRYGNLKNGVNDIKHKKWFATDWTIAIYQKQVEAPFIPKCKRGGDTSNFDDYEBEEDVRISST 341
 Octopus_bimaculoides VSGKVRFPSPHFSSDLKDLLRNLLQVDLTKRYGNLKNGVNDIKHKKWFATDWTIAIYQKQVEAPFIPKCKRGGDTSNFDDYEBEEDVRISST 341
 Lingula_anatina VSGKVRFPSPHFSSDLKDLLRNLLQVDLTKRYGNLKNGVNDIKHKKWFATDWTIAIYQKQVEAPFIPKCKRGGDTSNFDDYEBEEDVRISST 341
 Crassostrea_gigas VSGKVRFPSPHFSSDLKDLLRNLLQVDLTKRYGNLKNGVNDIKHKKWFATDWTIAIYQKQVEAPFIPKCKRGGDTSNFDDYEBEEDVRISST 341
 Biomphalaria_glabrata VSGKVRFPSPHFSSDLKDLLRNLLQVDLTKRYGNLKNGVNDIKHKKWFATDWTIAIYQKQVEAPFIPKCKRGGDTSNFDDYEBEEDVRISST 342
 Salmo_salar VSGKVRFPSPHFSSDLKDLLRNLLQVDLTKRYGNLKNGVNDIKHKKWFATDWTIAIYQKQVEAPFIPKCKRGGDTSNFDDYEBEEDVRISST 341
 Gallus_gallus VSGKVRFPSPHFSSDLKDLLRNLLQVDLTKRYGNLKNGVNDIKHKKWFATDWTIAIYQKQVEAPFIPKCKRGGDTSNFDDYEBEEDVRISST 344

Perinereis_aibuhitensis EKCAKEFAADF 350
 Aplysia_californica EKCAKEFAADF 352
 Xenopus_tropicalis EKCAKEFAADF 351
 Branchiostoma_floridae EKCAKEFAADF 369
 Danio_riero EKCAKEFAADF 351
 Octopus_bimaculoides EKCAKEFAADF 351
 Lingula_anatina EKCAKEFAADF 351
 Crassostrea_gigas EKCAKEFAADF 351
 Biomphalaria_glabrata EKCAKEFAADF 352
 Salmo_salar EKCAKEFAADF 351
 Gallus_gallus EKCAKEFAADF 354

Figure 7

The three dimensional structure of PKA from *P. aibuhitensis*.

The helix is colored by blue, the sheet is colored by magenta, and the loop is colored by salmon, DFG triplet is labeled in magenta.

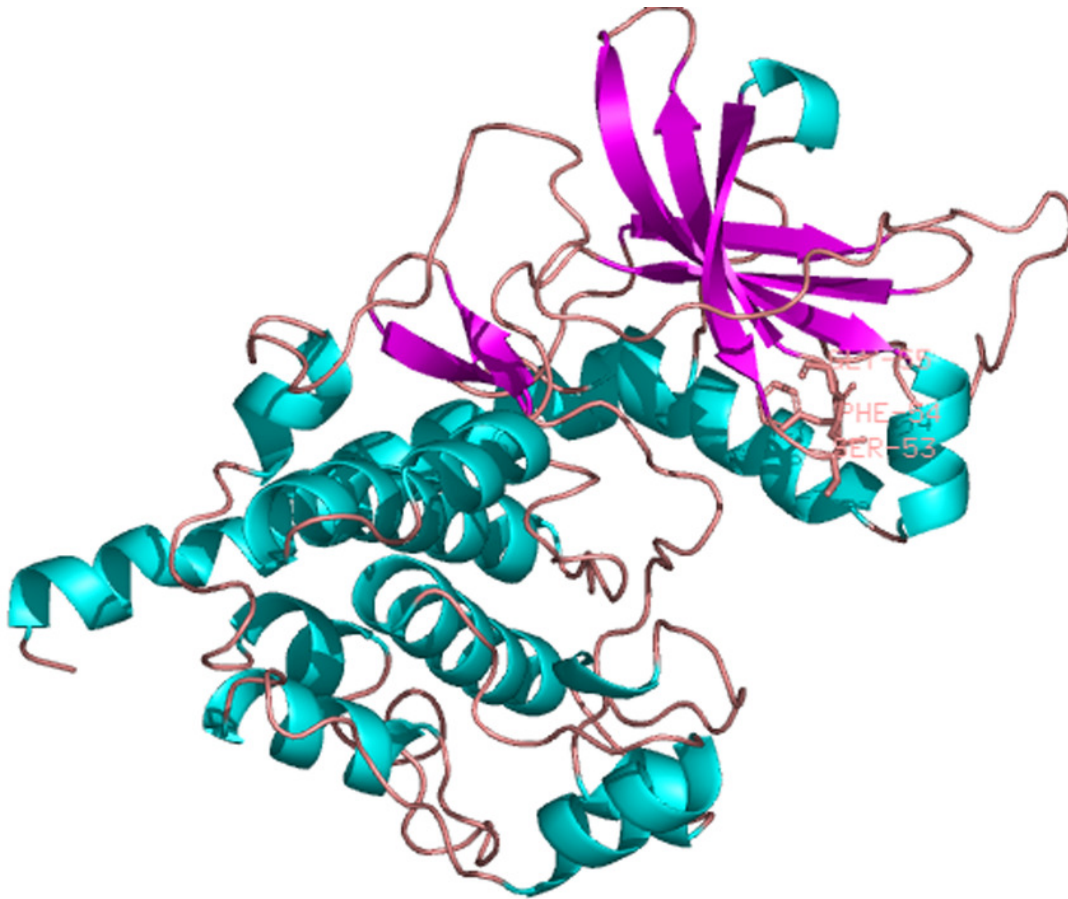


Figure 8

Phylogenetic analysis of PaGPCR related to GPCR of other invertebrates and vertebrates.

The information of other GPCR are same as the information in Figure 2; the tree topologies were evaluated with 1,000 replicates.

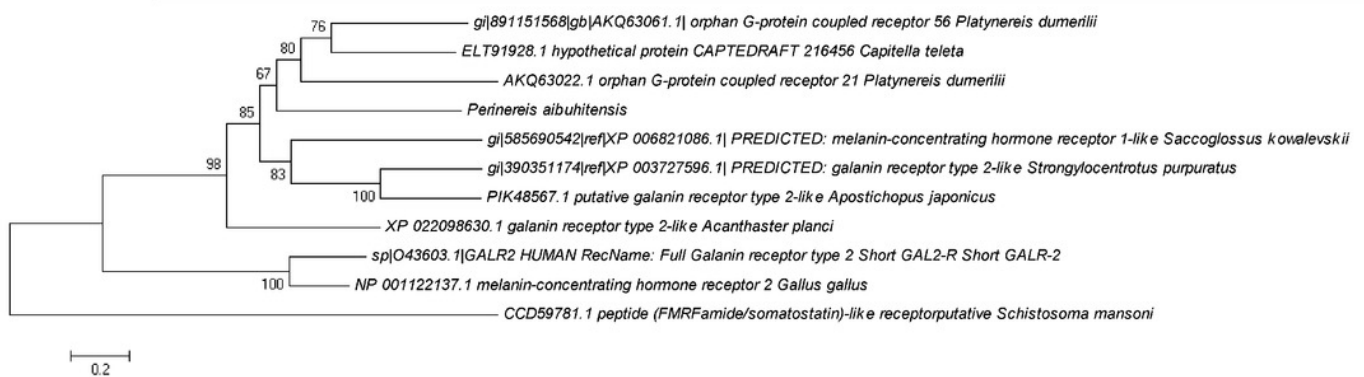


Figure 9

Phylogenetic analysis of PaPKA related to PKA of other invertebrates and vertebrates.

The information of other PKA sequence are as the information in Figure 6; the tree topologies were evaluated with 1,000 replicates.

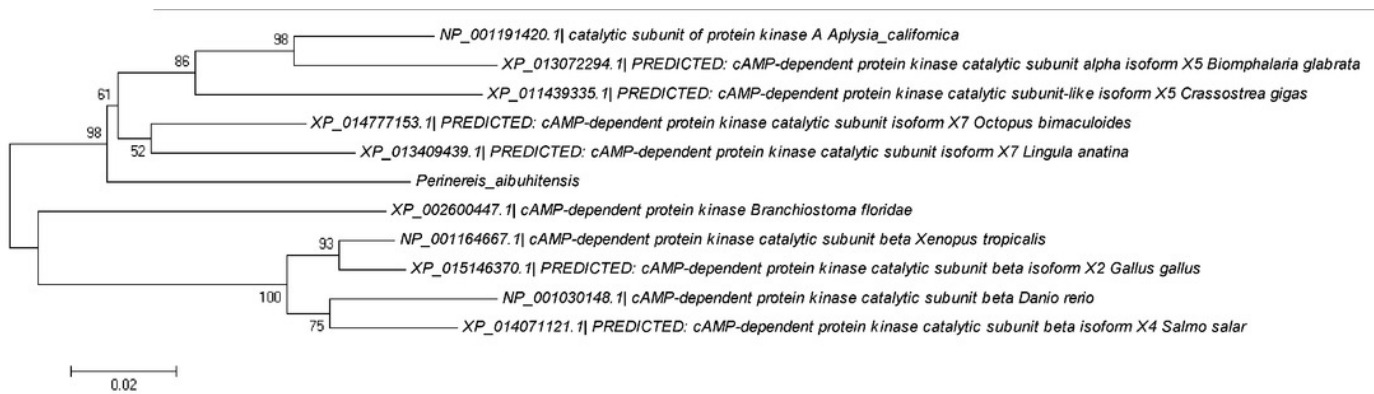


Figure 10

The relative expression level of *PaGPCR* and *PaPKA* cDNAs under various B(a)P concentration exposure.

A represents *PaGPCR*, B represents *PaPKA*. Different lowercase letters indicate significant difference ($P < 0.05$). all data as mean \pm SD. N = four worms.

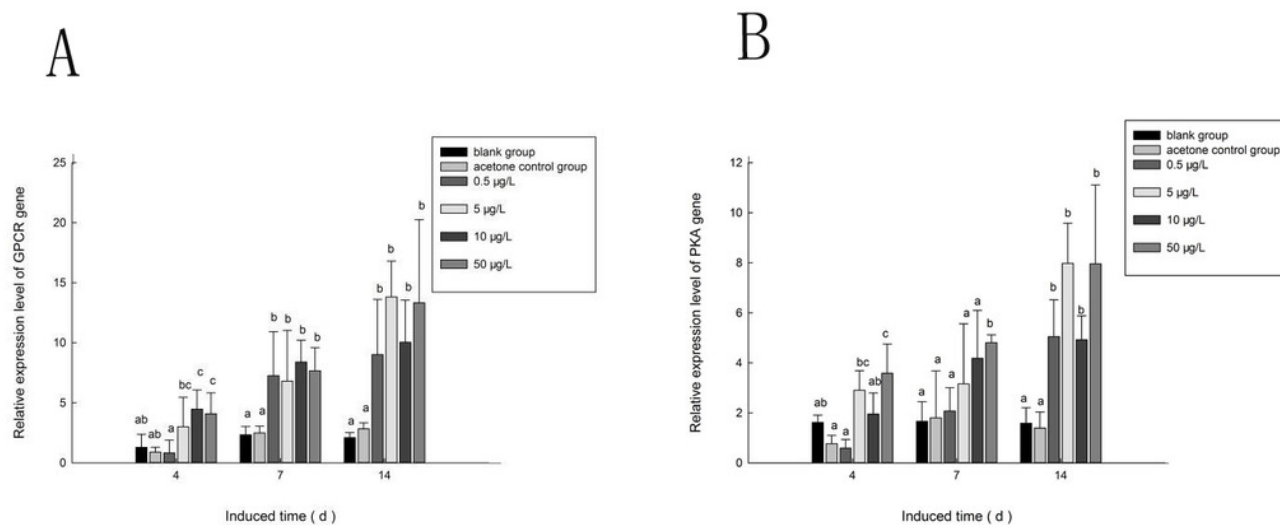


Figure 11

The PKA content under various B(a)P concentration exposure.

Different lowercase letters indicate significant difference ($P < 0.05$). all data as mean+SD. N= three worms.

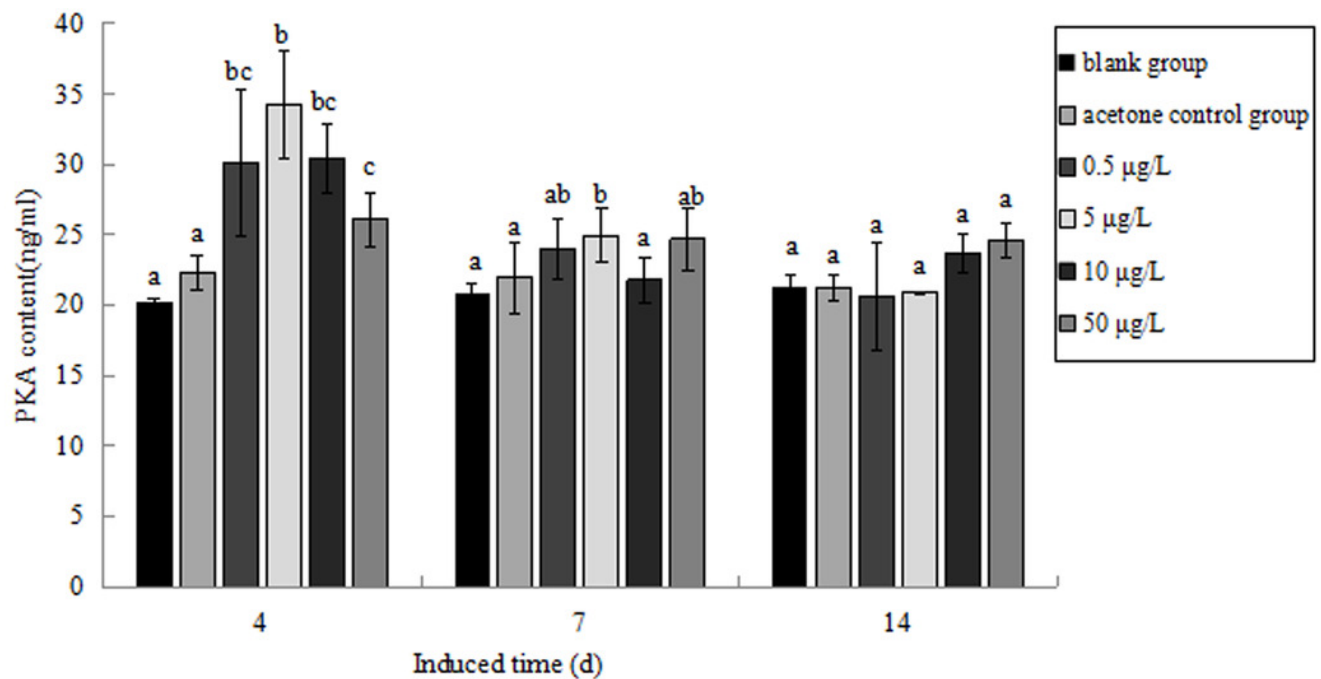


Table 1 (on next page)

The primers used in this study

Primer name		sequence (5'-3')
RACE	GPCR - F1	TGAGAAACGTCGAAGCGAAAGG
	GPCR - R1	ATATTCGACGCTGACCCTAAGG
	PKA-F1	GATACCCACCTTTCTTTGCTGACC
	PKA-F2	GGTGCGCTTCCCATCTCACTTT
	PKA-R1	CAATAGCGCAGCCTCAGGGACA
	UPM Long	CTAATACGACTCACTATAGGGCAAGCAG TGGTATCAACGCAGAGT
	UPM Short	CTAATACGACTCACTATAGGGC
Real time PCR	β -actin-R	CGAAGTCCAGAGCAACATAG
	β -actin-F	GGGCTACTCCTTCACCACCA
	GPCR-R3	CCGTAAAAGCCTCATCAAGACA
	GPCR-F3	TTGGCAGGTGTAAATGAATGG
	PKA-F3	GACCAGCCAATCCAAATCTATG
	PKA-R3	GACCCCATTCCTTCAGGTTTCC

1

2

3

4